

Heterotrinnuclear ring opening copolymerization catalysis: Structure-activity relationships

Alex J. Plajer^{a,†}, Charlotte K. Williams^{a,}*

^aUniversity of Oxford, Chemistry Research Laboratory, 12 Mansfield Road, OX1 3TA Oxford, United Kingdom; * charlotte.williams@chem.ox.ac.uk

CO₂ Copolymerization, Heteronuclear Catalysis, Polyols, Structure Activity Relationships

Abstract: Heteronuclear complexes are highly active catalysts in alternating ring opening copolymerizations (ROCOP) of cyclohexene oxide (CHO)/carbon dioxide or CHO/phthalic anhydride (PA). In this contribution, a series of new trinuclear complexes is investigated through a structure activity study that reveals the influences of ligand electronic and metal selection over the catalytic activity and linkage selectivity. The fastest catalyst shows high activity values for CHO/CO₂ ROCOP at low pressure (1 bar CO₂ pressure) and features the ligand coordinated to two Zn(II) centres and with inexpensive and abundant Na(I) (TOF = 1084 h⁻¹, catalyst:CHO 1:4000, 1 bar, 100 °C). High CHO/PA copolymerization activity is achieved with the combination of two Mg(II) and one Na(I) centre (TOF = 142 h⁻¹, catalyst:PA:CHO 1:200:4000, 100 °C), further the catalyst undergoes ‘switchable’ epoxide/anhydride ROCOP and epoxide ring opening polymerization (ROP), allowing for controlled ether linkage placement. Polymerization kinetic investigations reveal the influences of the ligand electronics, complex stability and metal-metal

separation and their influences over the retention of high activity throughout the catalysis. The findings should help to guide future polymerization catalyst design, facilitate novel block polymer production and may inspire other CO₂ utilization processes.

Introduction

Heteronuclear cooperativity has emerged as an important catalyst design concept and allows for improvement of activity beyond values achievable for homo-multinuclear metal catalysts.^{1,2} In polymerization catalysis, hetero-multinuclear complexes show real promise in lactone ring-opening polymerizations (ROP), olefin polymerizations and, relevant to this work, the ring-opening copolymerizations (ROCOP) of CO₂ or organic anhydrides with epoxides.^{3–9} However, not all metal combinations work equally well as some fail to act synergically and, consequently, better understanding of the phenomena underpinning catalytic catalysis is needed.^{10–12} One important open question is whether heteronuclear cooperative catalysts show the same degree of synergy when changing the substrate, for example from CO₂ to anhydride in ROCOP catalysis. Another series of questions concern how conventional ligand design and modification strategies affect internuclear cooperativity.

CO₂/epoxide copolymerization presents a viable option to transform globally accumulating waste CO₂ into useful polycarbonate materials, a range of different products and processes are being industrialized.^{13–18} Depending on the structures and molar mass values of the polycarbonates, different applications are feasible. Low molar mass hydroxyl-telechelic polycarbonates can serve as the diol/polyol components in polyurethane syntheses, forming products that show equivalent or better properties than those made using conventional polyether or polyester polyols.^{19–22} High molar mass CO₂-derived polycarbonates, in particular block or copolymers, may be applied as plastics, adhesives or elastomers.^{14,23–25} The ring-opening copolymerization process also applies

using cyclic anhydrides and epoxides; it offers an atom economical and generally applicable method to make a range of aliphatic, semi-aromatic and functionalized polyesters.^{7,26} These alternating polyesters can, for example, serve as a hard-blocks in degradable block polymer thermoplastic elastomers (TPE) where they raise the materials' upper operating temperatures compared against petrochemical SBS or SIS TPE.²⁷ Other alternating polyesters showed promise within fully bio-based and degradable pressure sensitive adhesives showing properties that matched successful petrochemical products.^{27,28} Both polycarbonates and polyesters may alleviate polymer sustainability concerns associated with hydrocarbon polymers containing stable but non-degradable C-C bonds.^{29,30} In contrast, ester and carbonate linkages can be cleaved, albeit under variable conditions which depend upon chemical structure, providing routes to degrade products fully to monomers/small-molecules, relevant for future chemical recycling and, in some cases, accelerating biodegradation/composting of the products.^{31–34}

Given the promise for these alternating polymers, it's important to continue to improve upon and better understand the polymerization catalysis. Bicomponent catalysts, comprising a Lewis acidic metal complex and nucleophilic cocatalyst, remain at the forefront of this field.^{3,4,7} Tethering the co-catalyst to the metal complex produces outstanding catalysts, but most of these require challenging ligand syntheses.^{35–39} An alternative approach is to modify reactivity by the correct placement of two or more metals within the ligand framework – these catalysts often function best without co-catalyst.⁴ High performance catalysts combining more than two metals are an exciting recent development, but understanding of how best to exploit multi-nuclear interactions remains in its infancy.^{40–49}

Recently a LMg(II)Co(II) CO_2/CHO ROCOP catalyst showed heterodinuclear synergy.^{50,51} Detailed kinetic analysis indicated that synergy correlated with a lower transition state entropy

barrier for Mg(II) containing catalysts and a lower transition state enthalpy barrier for Co(II) catalysts. Both effects are combined in the heterodinuclear Mg(II)Co(II) catalyst. It was hypothesized that in the rate determining step, the Mg(II) centre coordinates and orientates the incoming CHO monomer to attack by the Co(II)-carbonate nucleophile. Accordingly, catalytic synergy arises from each metal having a distinct ‘role’ in the rate determining step and by the two different metals providing optimized electronic requirements. These results motivate the broader exploration of other ligand scaffolds and multi-nuclear catalysts.^{52,53} We have recently reported a series of hetero-trinuclear LZnM catalysts (M = Li(I), Na(I), K(I), Ca(II), Sr(II), Y(III), La(III)) for either CHO/CO₂ or PA/CHO ROCOP.⁴⁰ Heterotrinuclear structures were delivered using a macrocyclic ligand featuring two bis(phenoxy)diimine binding pockets, i.e. coordination chemistry optimized for transition metals, and a central ‘cavity’ surrounded by six O-donor atoms suitable for the coordination of Group 1, 2 or lanthanide metals. The nature of the central metal M is important in determining whether CHO ROP, forming polyether (poly(cyclohexene oxide) PCHO), is also catalyzed. When the metal is sodium, controllable CHO ROP is combined with CO₂/CHO and PA/CHO ROCOP cycles to deliver block polymers. In these reactions, the CHO ROP occurs selectively *after* CO₂/CHO ROCOP and installs poly/oligoether end-groups to the chains which increase the polymer stability with respect to depolymerization compared with polycarbonate analogues. Here, we seek to investigate these hetero-trinuclear catalysts and understand the factors underpinning their performances. Considering how other epoxide/carbon dioxide ROCOP catalysts were improved shows that the electronic substituents on the ligand backbone can have a positive impact on catalyst performance. For example, electron-withdrawing substituents on bis(diketimide) or anilido-alimine macrocycles, coordinated to Zn(II), increased catalytic activity.^{54,55} In other work, changing the electronic nature on a non-initiating co-ligand

affected catalytic activity.⁵⁶ Therefore, it is of interest to investigate the influences of ligand electronic modification and the nature of the transition metals, in these trinuclear catalysts (Fig. 1).

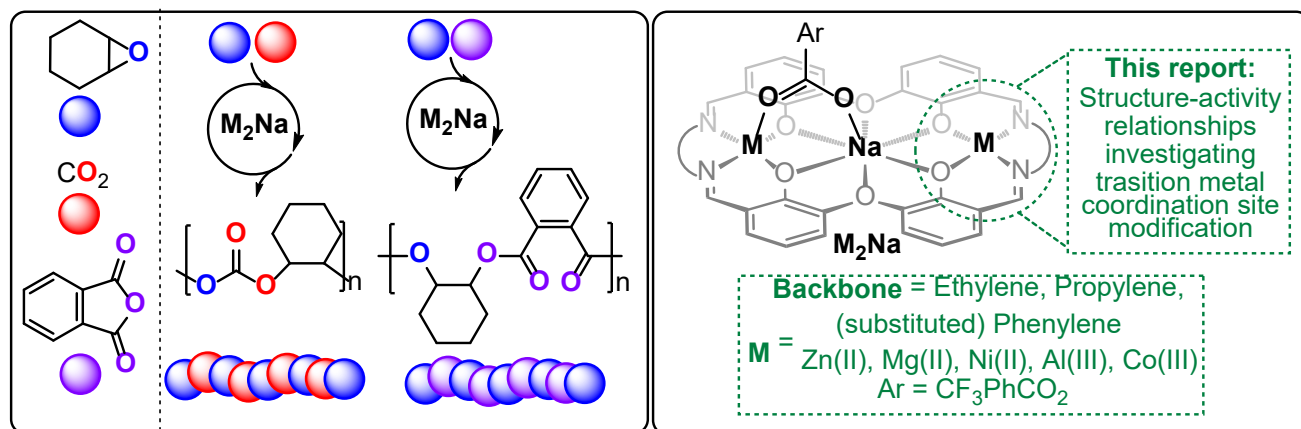


Figure 1: Structures of the monomers and catalysts used in CO₂/CHO and PA/CHO ROCOP.

Results

First, ligand backbone modifications were investigated, necessitating the preparation of ligands H₂L₁-H₂L₆ featuring different imine linker groups: ethylene, propylene, phenylene and substituted phenylenes featuring electron donating (methyl) and withdrawing (chloride and fluoride) groups (Fig. 2). The ligands were prepared by the condensation of dialdehyde precursor **A** with the appropriate diamines, yielding H₂L₁-H₂L₆ which crystallize or precipitate from the reaction mixture in pure form and good yields (see SI section S3 - S7). The series of new **Zn₂Na** coordination compounds (**1**_{ZnNa} - **6**_{ZnNa}) were synthesized in near quantitative yields by simultaneous reaction of each ligand with [Zn(OAc)₂(H₂O)₂] and NaCO₂C₆H₄CF₃. All complexes were yellow or red solids and were soluble in coordinating solvents, such as THF or DMSO, **5**_{ZnNa} also dissolves in chlorinated hydrocarbons.

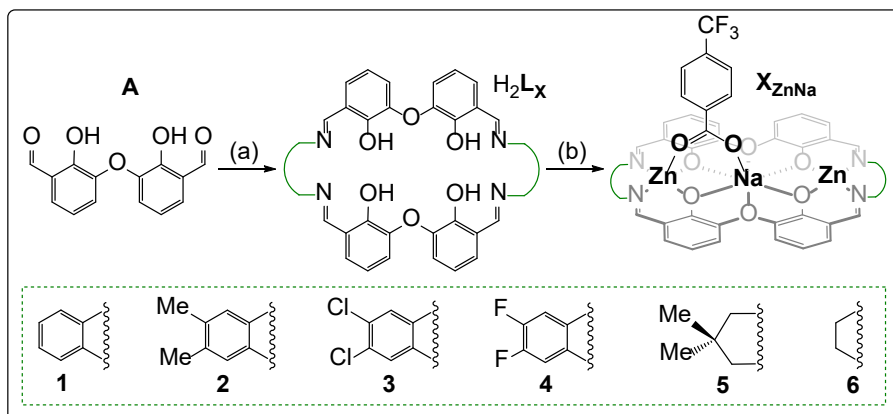


Figure 2: Synthesis of H_2L_1 - H_2L_6 from common precursor **A**, followed by the formation of catalysts **1**_{ZnNa} - **6**_{ZnNa}. Reagents and conditions: (a) 1 equiv. diamine, CH_3CN , room temperature, 1 h - 7 d, 25 - 77% yield (b) 2 equiv. $[Zn(OAc)_2(H_2O)_2]$, 1 equiv. $NaCO_2C_6H_4CF_3$, 1:1 CH_2Cl_2 :MeOH, room temperature, 5 - 60 min, 95 – 98% yield.

The complexes exhibit C_{4h} -symmetry on the NMR timescale, with 1H and $^{13}C\{^1H\}$ NMR spectra also indicating fast exchange of the benzoate co-ligands (see SI section S3 - S7). The benzoate group rapid exchange is indicated by broader phenylene resonances than for the sodium benzoate precursor and by the observation that addition of further $NaCO_2C_6H_4CF_3$ results in shifts to the averaged phenylene resonances for **1**_{ZnNa}-**6**_{ZnNa}. Catalyst **5**_{ZnNa} exhibits such a broad 1H NMR spectrum at room temperature that assignment is not feasible; this feature is attributed to its 2,2-dimethyl propylene backbone which was previously noted to cause similar spectroscopic broadening in other complexes. VT- 1H NMR spectroscopy of **5**_{ZnNa}, in d_2 -tetrachloroethane at temperatures up to 110 °C, results in sharper resonances consistent with C_{4h} symmetry. ESI-MS confirms the selective formation of hetero-trinuclear complexes, with a major ion consistent with $[X_{ZnNa} - CO_2C_6H_4CF_3]^+$ being observed in all cases. Elemental analyses confirm compositional purity and reveals the presence of water in some catalysts (direct coordination or lattice bound) similar to previous reports of related multi-nuclear complexes.⁵⁷⁻⁶⁰

The performance of each new complex in CO₂/CHO ROCOP catalysis was assessed (see SI section S3 - S7). The copolymerizations were monitored via *in situ* ATR-IR spectroscopy to accurately compare both reaction kinetics and product distributions. All the new complexes, except **6**_{ZnNa}, produced polycarbonates. The catalysts operate well at low loading, 0.025 mol% vs. CHO (catalyst:CHO = 1:4000), 1 bar CO₂ pressure and using excess chain transfer agent (20 equiv. of 1,2-cyclohexanediol, CHD). **Table 1** summarizes the CO₂/CHO ROCOP results and compares the results to leading catalysts in the field (Figure S2 illustrates the structures of these catalysts); more discussion of the activity context will be provided later in this paper.

Table 1: Data showing CO₂/CHO ROCOP performance of new catalyst investigated in this study and comparison with leading literature catalysts:

Cat. ^a	Polymer Selectivity (%) ^b	Carbonate: Ether (%) ^c	Polymer TON ^d	Polymer TOF [h ⁻¹] ^e	M _n [kg/mol] (Đ) ^f
[1 _{ZnNa}] ^g	97	86:14	1960	478	5.61 (1.29)
[2 _{ZnNa}]	95	82:18	1440	416	4.65 (1.22)
[3 _{ZnNa}]	97	95:5	800	310	3.01 (1.19)
[4 _{ZnNa}]	95	87:13	1956	1084	5.48 (1.18)
[5 _{ZnNa}]	91	78:22	1740	282	5.43 (1.23)
[6 _{ZnNa}]	Inactive				
[1 _{MgNa}]	62	99:1	314	16	n.d.
[1 _{AlNa}]	Decomposition				
[1 _{NiNa}]	Decomposition				
[1 _{CoNa}] [*]	99	73:27	520	270	2.0 (1.15)
[LMgZn(OAc) ₂] ^h	99	99:1	2280	295	8.0 (1.25)

[LMgCo(OAc) ₂] ⁱ	99	99:1	465	699	1.6 (1.15)
[L ₂ Zn ₂] ^j	98	99:1	1684	149	2.7 (1.28)
[LZn ₃ Ce(OAc) ₃] ^k	99	99:1	900	300	15.0 (1.2)
[LCo(X)] ^l	99	99:1	1315	263	48.2 (1.12)
[LCoNa(OAc) ₂] ^m	99	99:1	795	1590	5.3 (1.07)

^aCopolymerization conditions: 0.025 mol% catalyst loading (1:4000), 20 equiv. 1,2-cyclohexane diol (CHD), 1 bar CO₂, CHO neat (9.99 M), 100 °C (*80 °C). Polymerizations were stopped once conversion versus time plots deviate from linearity. ^bDetermined by comparison of the relative integrals, in the normalized ¹H NMR spectrum (CDCl₃, 25 °C), of resonances due to polymer (δ 4.65 ppm, 3.45 ppm) and cyclic carbonate (δ 4.00 ppm). ^cDetermined by comparison of the relative integrals, in the normalized the ¹H NMR spectrum, of resonances due to carbonate (δ 4.65 ppm) and ether (δ 3.45 ppm) linkages. ^dTurnover number (TON), number of moles of CHO consumed per mole of catalyst. ^eTurnover frequency (TOF) determined from initial rates analysis by in situ ATR-IR spectroscopy (typically 5 – 15% conversion) as TON/time. ^fDetermined by GPC (gel permeation chromatography) measurements conducted in THF, using narrow MW polystyrene standards to calibrate the instrument; $\bar{D} = M_w/M_n$. ^gAccording to Reference ⁴⁰. ^hLiterature catalysts tested at 0.05 mol% catalyst and 100 °C; for more details see reference ⁶¹. ⁱLiterature catalysts tested at 0.05 mol% catalyst and 100 °C; for more details see reference ⁵⁰. ^jLiterature catalyst tested at 0.1 mol% and 100 °C; for more details see reference ⁶². ^kLiterature catalysts tested at 0.05 mol% catalyst, 3 bar CO₂ pressure and 100 °C; for more details see reference ⁴¹. ^lLiterature catalysts tested at 0.02 mol% and 50 °C; for more details see reference ⁶³. ^mLiterature catalyst tested at 0.025 mol%, in presence of 10 equiv. CHD and 100 °C; for more details see reference ⁵². Note that “L” in this table abbreviates different sets of ligand, see Figure S2 for structures of the catalysts.

Catalyst **4_{ZnNa}**, which features a difluorophenylene backbone, shows the highest activity and achieves a TOF value of 1083 h⁻¹ (**Table 1**, #4). Catalysts featuring either more electron rich or electron poor backbones show decreased activity. The catalyst activity peaks at the mid-point moving from electron rich to electron poor backbones (i.e. order **5_{ZnNa}** < **6_{ZnNa}** < **2_{ZnNa}** < **1_{ZnNa}** < **4_{ZnNa}** < **3_{ZnNa}**) (**Figure 2**). It is proposed that electron poor backbones enhance epoxide activation in the rate determining transition state, yet they may also strengthen the coordination of the propagating carbonate bond and hence reduce its reactivity towards insertion reactions. Therefore, it seems there is an optimum balance in metal electronic properties when varying the ligand backbone electronic features. This observation substantiates the hypothesis that the exterior Zn(II) centers simultaneously fulfill two roles in the rate determining step of the catalysis.

Another clear trend is that electron rich ligand backbones cause more ether linkages in the polycarbonates (**Table 1**). It was previously established that ether linkages form as a result of a rapid carbonate insertion/ CO_2 extrusion equilibrium.⁴⁰ For 1_{ZnNa} , CO_2 fixation is temperature dependent, and Van't Hoff analysis showed exothermic, but endotropic, CO_2 insertion (see **Figure 2**). It is proposed that carbon dioxide insertion occurs many times faster than epoxide insertion in the main propagation cycle, causing rapid equilibration between carbonate and alkoxide resting states from which rate determining epoxide insertion occurs. Consistent with this prior work, the data correlating ligand backbones to ether linkage selectivity in this work indicate that electron poor backbones result in equilibria which are shifted towards the carbonate intermediate and hence show reduced ether linkage formation.

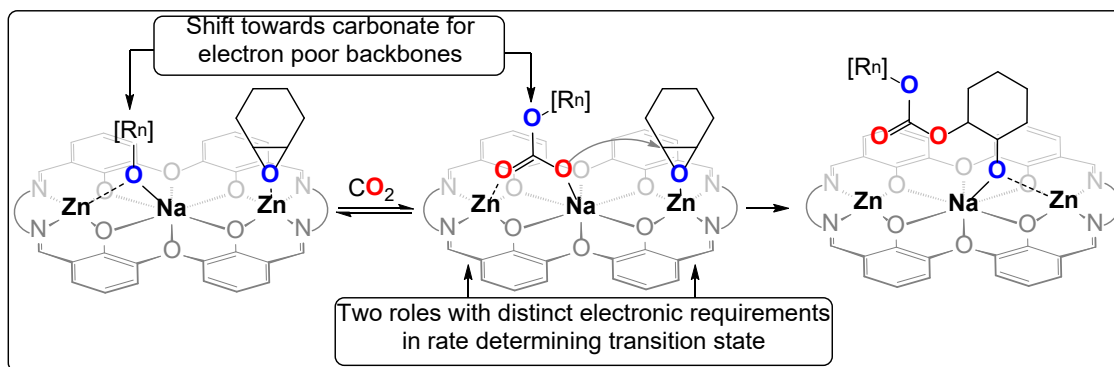


Figure 3: Diagram illustrating some of the factors which may underlie catalyst activity and selectivity.

The same catalysts were tested for the mechanistically related PA/CHO ROCOP and similar activity trends were observed, but with some differences (see SI section S3 - S7). The catalysts were tested using a set of demanding conditions (1:20:200:4000, catalyst:CHD:PA:CHO, neat CHO, 100 °C). All the catalysts were active and yielded alternating polyesters without any ether linkages. Catalysts featuring phenylene backbones performed well ($\text{ToF} = 92 - 225 \text{ h}^{-1}$) and the best catalyst 3_{ZnNa} ($\text{ToF} = 225 \text{ h}^{-1}$) features electron withdrawing chloride substituents on the

phenylene backbone. Catalyst **6_{ZnNa}** which was inactive in CO₂/CHO ROCOP, showed moderate activity for PA/CHO ROCOP (ToF = 50 h⁻¹), exceeding that of **5_{ZnNa}** (ToF = 6 h⁻¹). Catalysts featuring aliphatic backbones were less active than aromatic ones just like for CO₂/CHO ROCOP. Taken together it can be seen that structural and electronic requirements for high ROCOP performance in PA/CHO and CO₂/CHO ROCOP are related but not precisely matching for these heterotrinnuclear catalysts, suggesting similarity in the two catalytic cycles.

Table 1: Data showing PA/CHO ROCOP performance of new catalyst investigated in this study and comparison with leading literature catalysts:

Cat. ^a	Ester selectivity	PCHPE TON	PCHPE TOF [h ⁻¹] ^b	M _n [kg/mol] (Đ) ^c
[1_{ZnNa}] ^d	>99 %	200	173	-
[2_{ZnNa}]	>99 %	200	120	2.26 (1.18)
[3_{ZnNa}]	>99 %	200	225	1.90 (1.17)
[4_{ZnNa}]	>99 %	200	92	2.05 (1.16)
[5_{ZnNa}] [†]	>99 %	100	6	1.05 (1.16)
[6_{ZnNa}]	>99 %	200	50	1.75 (1.15)
[1_{NiNa}]	Decomposition			
[1_{AlNa}]	Decomposition			
[1_{CoNa}] [*]	>99 %	200	136, 51	2.23 (1.17)
[1_{MgNa}]	>99 %	200	142	3.97 (1.19)
[LMg₂(OAc)₂] ^e	>99 %	100	35	17.0 (1.08), 8.7 (1.11)
[LMgNa(OAc)] ^e	>99 %	100	10	21.5 (1.13), 9.8 (1.08)
[LZn₂(OAc)₂] ^e	>99 %	99	198	5.3 (1.23)
[LMg₂(OAc)₂] ^f	>99 %	97	97	12.7 (1.10), 5.5 (1.06)

[Urea/PPNCl] ^g	>99 %	76	456	7.6 (1.19)
[(LAICl) ₂ /2 PPNCl] ^h	>99 %	225	750	9.8 (1.14)
[LFe ₂ /PPNCl] ⁱ	>99 %	290	1180	7.3 (1.24)
[R ₄ NCl-tethered-BR ₃] ^j	>99 %	172	258	24.5 (1.18)
[LAIK(OAc)] ^k	>99 %	268	1072	14.3 (1.06)
[(LCrCl) ₃ /3 PPNCl] ^l	>99%	3540	10620	12.3 (1.21)
[LCrCl/PPNCl] ^m	>99%	97	1160	5.1 (1.17)

^aCopolymerization conditions: 0.025 mol% catalyst loading (1:4000), 20 equiv. 1,2-cyclohexane diol (CHD), 200 equiv. PA ([†]100 equiv.), CHO neat (9.99 M), 100 °C. *80 °C, two TOF values are reported – the first prior to and the second post thermal reduction. Polymerizations were stopped once CHO to PCHO conversions versus time plots deviate from linearity, after complete PA consumption. ^bTurnover frequency (TOF) determined from rate analysis by *in situ* ATR-IR spectroscopy (typically 20 – 80% PA conversion) as TON/time. ^cDetermined by GPC (gel permeation chromatography) measurements conducted in THF, using narrow MW polystyrene standards to calibrate the instrument; $\bar{D} = M_w/M_n$; note that molecular weights differ due to differing extents of CHO ROP occurring after PA/CHO ROCOP as evident from the *in situ* ATR-IR spectroscopy (SI). ^d According to reference ⁴⁰. ^e Literature catalysts tested at 1 [Cat.]: 100 [PA] : 1000 [CHO] at 100 °C; for more details see reference ¹². ^f Literature catalysts tested at 1 [Cat.]: 100 [PA] : 800 [CHO] at 100 °C; for more details see reference ⁶⁴. ^g Literature catalysts tested at 1 [Cat.]: 100 [PA]: 200 [CHO] at 100 °C; for more details see reference ⁶⁵. ^h Literature catalysts tested at 1 [Cat.]: 250 [PA]: 1000 [CHO] at 100 °C; for more details see reference ⁶⁶. ⁱ Literature catalysts tested at 1 [Cat.]: 500 [PA]: 2500 [CHO] at 100 °C; for more details see reference ⁶⁷. ^j Literature catalysts tested at 1 [Cat.]: 200 [PA]: 400 [CHO] and 120 °C; for more details see reference ⁶⁸. ^k Literature catalysts tested at 1 [Cat.]: 400 [PA]: 2000 [CHO] at 100 °C; for more details see reference ⁶⁹. ^l Literature catalysts tested at 1 [Cat.]: 6000 [PA]: 30,000 [CHO] at 100 °C; for more details see reference ⁴⁶. ^m Literature catalysts tested at 1 [Cat.]: 100 [PA]: 500 [CHO] at 100 °C; for more details see reference ⁷⁰. Note that “L” in this table abbreviates different sets of ligand, see Figure S2 for structures of the catalysts.

In contrast to CO₂/CHO ROCOP, no random ether linkages were observed during PA/CHO ROCOP. Monitoring the polymerizations using *in situ* ATR IR spectroscopy reveals a zeroth order in anhydride concentration, after a short induction period (see e.g. Figure S12). These data suggest that PA insertion is significantly faster than CHO insertion and because the carboxylate linkage formed after insertion is not in equilibrium with the alkoxide so there is high polyester selectivity. The reaction monitoring does reveal that catalysts with aromatic backbones, switch from PA/CHO

ROCOP to CHO ROP once the PA is consumed. This second process forms polyether (PCHO) end groups on the telechelic polyester chains. Such reactivity contrasts with most other catalysts reported in the literature which are selective only for PA/CHO ROCOP (see Figure S3). Investigation of the CHO ROP indicates it likely operates by a coordination-insertion mechanism since the resulting PCHO has low dispersity ($\mathcal{D} < 1.3$), whereas cationic epoxide ROP usually produces polyether showing broad molar mass dispersity.^{40,71,72} The polymerization mechanistic switch (from CHO/PA ROCOP to CHO ROP) does not occur for the aliphatic backbone linker catalysts **5**_{ZnNa} and **6**_{ZnNa}. This observation is somewhat surprising because **5**_{ZnNa} does produce random ether linkages in the CO₂/CHO ROCOP polymer. For CO₂/CHO catalysis using **5**_{ZnNa} it could be tentatively proposed that the coordination of the carbonate linkages adjacent to the alkoxide chain end facilitates the subsequent ether linkage formation. In the PA/CHO ROCOP case, the less coordinating and more rigid aryl ester groups seem less likely to coordinate and this may be a rationale for why CHO homopropagation is not observed. Such a rationale bears similarity to the selectivity recently observed in Sn(II) epoxide/anhydride ROCOP catalysts where alternating ester-ether linkages (ABB patterns) form.^{73,74}

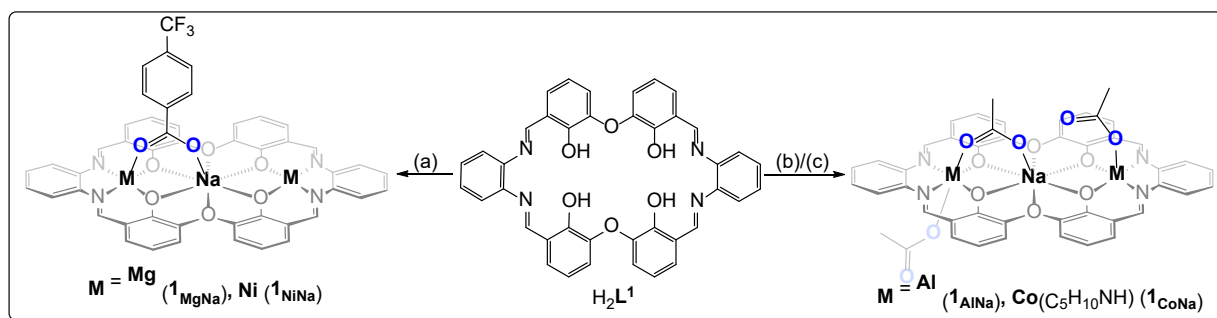


Figure 3: Synthesis of catalysts **1**_{MgNa}, **1**_{NiNa}, **1**_{CoNa}, **1**_{AlNa}. Reagents and conditions: (a) 2 equiv. [M(OAc)₂(H₂O)_x] (M = Mg(II), Ni(III)), 1 equiv. NaCO₂C₆H₄CF₃, 1:1 CH₂Cl₂:MeOH, RT, 60 min; 94 - 96% yield (b) (i) 2 equiv. AlEt₃, THF, RT, 16 h; (ii) 2 equiv. HOAc, THF, RT, 5 h; (iii) 1

equiv. NaOAc, MeOH, RT, 5 min, 46% yield over 3 steps. (c) (i) to **1_{Co}** according to Akine and coworkers as per reference⁷⁵, (ii) NaOAc, MeOH, RT, 1 min, quantitative.

Next, the investigation turned to the influences of changing the ‘external’ metals, M, coordinated by the bis(phenoxy)diimine pockets of the ligand, H₂L¹. The Ni(II) **1_{NiNa}** and Mg(II) **1_{MgNa}** catalysts were obtained in near quantitative yields (>95%) via a simultaneous metalation method of synthesis (Fig. 3) (see SI Section S8 and S9). Treatment of H₂L¹ with Et₃Al, followed by addition of both acetic acid and sodium acetate yielded the aluminium catalyst **1_{AlNa}** (see SI Section S10). Reaction of the dicobalt(III) acetate complex of L¹ (**1_{Co}**), recently reported by Akine and coworkers, with sodium acetate yielded the cobalt(III) catalyst **1_{CoNa}** (see SI Section S11).⁷⁵ All the complexes show *C*_{4h} symmetry, as indicated by ¹H NMR spectra with broadened benzoate or acetate resonances, suggesting fast exchange of the carboxylate groups. Catalysts **1_{NiNa}** and **1_{AlNa}** were inactive in CO₂/CHO ROCOP and decomposed after ca. 30% PA conversion in PA/CHO ROCOP, as evident from *in situ* ATR-IR spectroscopic monitoring (see SI Figure S56 and S60). For catalyst **1_{AlNa}** cessation of PA/CHO ROCOP coincides with the emergences of a bright red colour. Such colour changes are characteristic of the formation of alkoxide intermediates in the catalytic cycle.^{40,76} Hence it is proposed that the catalyst decomposition originates from alkoxide intermediate instability. In the case of **1_{MgNa}**, CO₂/CHO ROCOP proceeded slowly (ToF = 16 h⁻¹, Table 1) producing perfectly alternating PCHC, albeit in only 62% polymer selectivity alongside cyclic carbonate (see SI Figure S50). This result could indicate of weaker coordination of the propagating chain end to the Mg(II) centres. Such a notion correlates with the Irving-Williams metal reactivity series which predicts that Zn(II) complexes are more stable towards ligand dissociation than Mg(II) complexes.⁷⁷ Less strongly coordinated metal-polymer chain ends may give rise to backbiting side reactions during CO₂/CHO ROCOP and reduce the polymer selectivity.

Interestingly **1**_{Co}, that is **1**_{CoNa} prior to acetate coordination, is inactive in CO₂/CHO ROCOP. As can be seen in the single crystal X-ray structure of **1**_{Co}, published by *Akine* and coworkers, the two Co(III) centres are separated by 7.32 Å.⁵⁸ The inclusion of the additional sodium centre reduces the internuclear distance (here Co-Na) to ~ 3.45 Å as observed in the X-ray structure of the NaOTf complex of **1**_{Co}, again reported by *Akine* and co-workers.⁷⁵ Thus, **1**_{CoNa} (the NaOAc complex of **1**_{Co}) is active in CO₂/CHO ROCOP (TOF 270 h⁻¹ at 80 °C, 99% polymer selectivity, 73% PCHC and 27% PCHO). It is proposed that there is an optimal metal-metal distance in this catalysis likely due to the need for epoxide coordination and reverse side attack by an adjacent metal-nucleophile. A prior DFT analysis of the propagation of PO/CO₂ polymerization, using heterogenous zinc glutarate catalysts, also proposed a similar optimum inter-Zn(II) distance of 4.3–5.0 Å on the catalyst surface.⁷⁸ The structural requirements previously identified for heterogenous CO₂ ROCOP catalysts appear to be similar for these homogeneous hetero-trinuclear complexes. Moreover, **1**_{CoNa} was observed to be thermally unstable; conducting CO₂/CHO ROCOP at 100 °C led to very low maximum CHO conversion < 5%. The thermal decomposition was slowed at lower temperatures, so decreasing the polymerization temperature to 80 °C resulted in a maximum CHO conversion of ca. 15% (see Figure S63). Nevertheless, even at 80 °C decomposition still occurs as stable Zn catalysts achieve maximum conversions of close to 50% under equivalent conditions. Previous reports note that Co(III) ROCOP catalyst tend to suffer with low thermal stability due to irreversible cobalt redox transitions.^{79,80} Monitoring the PA/CHO ROCOP using **1**_{CoNa} by *in situ* IR spectroscopy at 80 °C showed a distinct decrease in catalytic activity over time which is attributed to reduction of the Co(III) centres in **1**_{CoNa} to less active Co(II) species (see Figure S64).

Finally, catalyst **1**_{MgNa} performed very well in PA/CHO ROCOP (ToF 142 h⁻¹, Figure 3) and showed a zeroth order rate dependence in PA concentration, as seen by *in situ* IR spectroscopy

monitoring (see Figure S51). After complete PA conversion, **1**_{MgNa} was switched into rapid CHO ROP (ToF = 511 h⁻¹). This results in the formation of telechelic polyester chains which are appended with two polyether end-caps. Ether formation is controlled, as confirmed by narrow monomodal molecular weight distribution ($\mathcal{D} < 1.2$). A previous study employing **1**_{ZnNa} in PA/CHO ROCOP to CHO ROP switchable catalysis suggested that the mechanistic switch correlated with a change in the catalyst resting state from a metal-carboxylate to an alkoxide intermediate. This was indicated by the solution colour: a darkening of the reaction mixture from orange (carboxylate) to brown (alkoxide) was observed for **1**_{ZnNa}. Here, a similar colour change from yellow (carboxylate intermediate) to brown (alkoxide intermediate) was also observed during the switch in mechanism for catalyst **1**_{MgNa} suggesting that the reaction colour, once again, correlates with a change from metal carboxylate to alkoxide resting state.

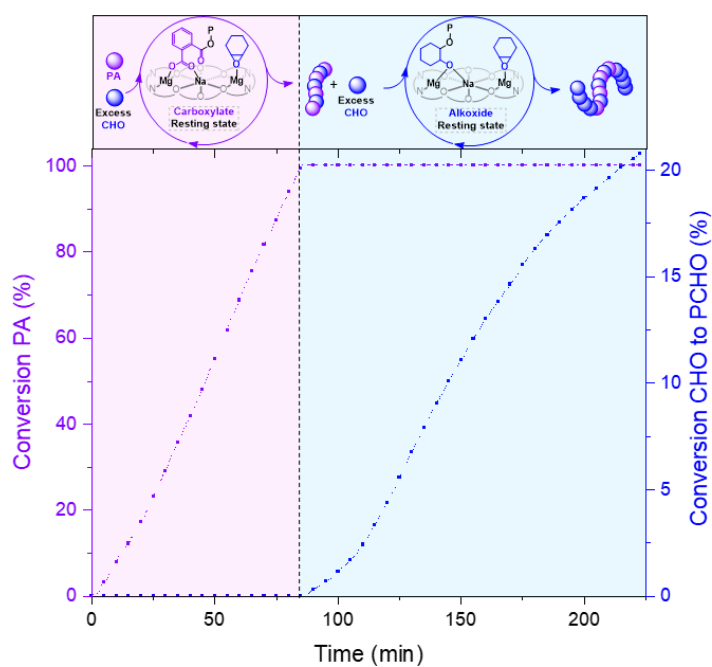


Figure 4: Conversion vs time plot obtained via in situ ATR-IR spectroscopic monitoring of PA/CHO ROCOP, followed by CHO ROP after ca. 80 min (reaction conditions: 1 equiv. **1**_{MgNa} : 20 equiv. CHD: 400 equiv. PA: 4000 equiv. CHO, 100 °C).

Discussion

Comparing the new heterotrinnuclear catalysts against the best literature catalysts is necessary to appreciate the performance benefits. However, such comparisons are not straightforward as catalysts tend to be tested under different conditions in different laboratories (catalyst loading, CO₂ pressure, reaction temperature, presence of chain transfer reagent). For CO₂/CHO ROCOP, there are two general classes of catalysts: (i) Those operating at low CO₂ pressure (< 3 bar), for example the complexes presented in this study and which can thus be used in non-specialist laboratory glassware and (ii) those operating at high CO₂ pressure (typically >10 bar) which require specialist steel reactor equipment and mechanical stirring. Table 1 compares the catalysts reported in this study to other high activity CO₂/CHO ROCOP catalysts operating at low CO₂ pressure and low loading, at 100 °C and, if possible, in presence of chain transfer reagent. The Zn₂Na catalysts all show high activities, the fastest catalyst **4**_{ZnNa} shows a TOF of 1084 h⁻¹ which is at the upper end in this class of catalysts. Other high activity catalysts include two heterodinuclear complexes, LCo(III)Na(I) with a TOF of 1590 h⁻¹ (100 °C, 0.025 mol%) and LCo(II)Mg(II) with a TOF of 699 h⁻¹ (100 °C, 0.05 mol%) (see Figure S2 for illustrations of the structures of these catalysts).^{50,52} These two literature catalysts feature different ancillary ligands and both apply cobalt as part of the active site. There may be advantages, especially in terms of colour and earth-abundance, to catalysts based on zinc, alkali and lanthanide metals. Another point of difference lies in catalytic selectivity: these heterotrinnuclear catalysts form poly(carbonate-ran-ether) whilst almost all other

literature catalysts produce polycarbonates featuring > 99% carbonate linkages. It is already clearly established that high pressure catalysts, and those conducted using mechanical stirring, tend to show much higher activities.^{3,4} This means there are many high-pressure CO₂ ROCOP catalysts that can outperform **4**_{ZnNa}. Leading catalysts under these conditions include those reported by: Rieger and co-workers with a **L**Zn₂(N(TMS₂))₂ catalyst with a TOF of 155,000 h⁻¹ (0.0125 mol%, 100 °C, 30 bar CO₂, 85% carbonate links); Nozaki and co-workers reported an ammonium tethered **L**Al(III)Cl porphyrin complex with a TOF of 10,000 h⁻¹, (0.0025 mol%, 120 °C, 20 bar CO₂, 99% carbonate links); Wu and co-workers prepared an ammonium tethered borane [R₄NCl-tethered-BR₃] with a TOF of 4900 h⁻¹ (0.02 mol%, 150 °C, 15 bar CO₂, 99% carbonate links) and we reported a **L**Co(II)Mg(II) catalyst, coordinated by a different macrocycle, with a TOF of 12,460 h⁻¹ (0.05 mol%, 140 °C, 20 bar CO₂, 99% carbonate links).^{39,50,55,81} In future these new heterotrinnuclear catalysts could be tested under high CO₂ pressure to explore fully the upper limits in terms of activity and selectivity.

Comparing these new catalysts with other known PA/CHO ROCOP catalysts is also challenging due to a lack of field standardization of conditions (Table 2). Where possible, comparisons are made at 100 °C, in neat CHO and PA loadings of 100 – 500 equiv. of anhydride per catalyst (see Figure S3 for precise conditions). Again, catalysts are classified into two sets: (i) Bicomponent catalysts (those where PPNCI or other co-catalysts are added separately) and (ii) Monocomponent catalysts, including multi-nuclear complexes or tethered catalysts. These latter typically maintain performances even under increasing catalyst dilution. Although bicomponent catalysts (i) show high activity and selectivity, they rely on intermolecular association and, therefore, generally require higher catalyst loadings.³⁵ Furthermore, type (ii) catalysts generally tolerate the presence

of excess chain transfer agent (as is the case here) which is attractive because this it produces both low and high molecular weight polymers and fully controls end-group chemistry.³⁸ The best PA/CHO ROCOP catalyst, **3**_{ZnNa} (TOF = 225 h⁻¹ at 0.025 mol% vs CHO) shows an activity at the upper end of class (ii) species. It is only surpassed by an Al(III)K(I) catalyst very recently reported by our team (TOF = 1072 h⁻¹ at 0.05 mol% vs CHO),⁶⁹ and by a trinuclear Cr(III) salen species, activated with three equivalents of PPNCI, reported by Lu and co-workers which showed an outstanding activity (TOF = 10620 h⁻¹ at 0.0033 mol% vs CHO).⁴⁶ One future area to explore would be to apply the trinucleating salen ligand, used by the Lu group and others, to make mixed metal catalysts.

The high activity combined with the unusual selectivity of **1**_{MgNa} is also worth note. Previously, a binuclear **LMg(II)Na(I)** catalyst, coordinated by a different macrocycle, showed ~ ten times lower activity in PA/CHO ROCOP than **1**_{MgNa} and showed no activity in CHO ROP under equivalent conditions.¹² This result highlights how apparently minor modifications to the ligand can result in step-changes to both activity and selectivity. Group 1 and 2 metal chemistry is worth exploring further in catalysis because of sustainability and economic concerns associated with transition metals.^{1,82} Regarding the selectivity switch, very few other catalysts are able to change polymerization cycle from PA/CHO ROCOP to CHO ROP. The only prior examples are a catalyst in this family, **1**_{ZnNa}, and a bicomponent BEt₃/^tBuP₂ catalyst.^{25,40,83} Compared to the latter organocatalysts system, **1**_{MgNa} operates at significantly lower catalyst loading (0.5 mol% for BEt₃/^tBuP₂ compared to 0.025 mol% for **1**_{MgNa} with respect to CHO). Curiously, **1**_{MgNa} also achieves a higher CHO conversion than **1**_{ZnNa} (see Figure S52). While BEt₃/^tBuP₂ (TON = 4; TOF = 0.3 h⁻¹; 2% final turnover of initial feed at 60°C) and **1**_{ZnNa} (TON = 640, TOF = 500 h⁻¹; 16% final turnover

of initial feed at 100°C) reach only modest conversions, **1_{MgNa}** achieves a CHO conversion of 50% equating to a TON of 2000 (TOF = 240 h⁻¹). This increased conversion yields higher degrees of polymerization within the PCHO end-blocks. It is attributed to the higher stability, during CHO ROP, of **1_{MgNa}** compared with **1_{ZnNa}**. The ability to control the PCHO block molar mass/DP could be important for any future explorations of these block polymers and could even be relevant to achieving phase separation.²⁵ Therefore, **1_{MgNa}** is likely to be the more attractive self-switchable catalyst for future material synthesis.

Conclusions

High activity heterotrinnuclear catalysts, coordinated by a macrocyclic ligand featuring two Schiff base binding ‘pockets’ and a central O-donor pocket, were developed for CO₂/CHO and PA/CHO ROCOP catalysis. The catalysis requires a fine balancing of the ancillary ligand electronic profile, an optimal intermetal distance and sufficient metal centre stability. Within the series of catalysts, the central metal was maintained as sodium due to its earth-abundance and low cost, whilst the two exterior metals and ligand framework were systematically modified. The results indicate that the two exterior metals serve two functions in catalysis, namely epoxide activation at one metal and chain-end coordination at the other. Upon investigating the exterior metals, the highest activity and selectivity was observed for the catalyst featuring Zn₂Na as the metal combinations. Using the Zn₂Na metal combination and changing the imine linker group showed that the most active and selective catalyst featured a 1,2-difluoro-phenylene moiety. Overall, the best dizinc-sodium catalyst showed very high activity, with a TOF > 1000 h⁻¹, in low pressure CO₂/CHO ROCOP catalysis. The finding is significant as it diversifies the range of high performance ligands and metals feasible in this field. The same catalysts showed related

performances in PA/CHO ROCOP, with complexes featuring phenylene linker groups having higher activity than aliphatic backbones. Once again, the two exterior metals are optimal for Zn(II) compared with Mg(II), Co(III), Ni(II) or Al(III) counterparts, under equivalent conditions. The Zn_2Na and Mg_2Na catalysts showed an unusual mechanistic switch during catalysis and formed poly(ester-b-ether) structures. Considering this switchable catalysis, the best catalyst featured $\text{Mg}(\text{II})_2\text{Na}(\text{I})$, likely due to its greater stability during the epoxide ring-opening catalysis. Overall, these new heterotrinnuclear catalysts highlight the potential for s-block metals in this field of catalysis which has traditionally been dominated by a limited range of first row transition metals. In future, ligand diversification should continue with focus on structures suitable for s-block metal coordination and these catalysts should be explored in other polymerizations and carbon dioxide utilizations.

Corresponding Author

* charlotte.williams@chem.ox.ac.uk

Present Addresses

† Freie Universität Berlin, Institut für anorganische Chemie, Fabeckstraße 34/36, 14195 Berlin, Germany

Author Contributions

The manuscript was written through contributions of all authors. All authors have given approval to the final version of the manuscript.

Funding Sources

The EPSRC (EP/S018603/1; EP/R027129/1), the Oxford Martin School (Future of Plastics) and the Royal Commission for the Exhibition of 1851 (Research Fellowship for A. J. P.) are acknowledged for funding.

References

- 1) Gil-Negrete, J. M.; Hevia, E. Main Group Bimetallic Partnerships for Cooperative Catalysis. *Chem. Sci.* **2021**, *12* (6), 1982–1992..
- (2) Mata, J. A.; Hahn, F. E.; Peris, E. Heterometallic Complexes, Tandem Catalysis and Catalytic Cooperativity. *Chem. Sci.* **2014**, *5* (5), 1723–1732.
- (3) Trott, G.; Saini, P. K.; Williams, C. K. Catalysts for CO₂/Epoxide Ring-Opening Copolymerization. *Philos. Trans. R. Soc. London Ser. A* **2016**, *374* (2061), 20150085.
- (4) Williams, C. K.; Plajer, A. J. Heterocycle/Heteroallene Ring Opening Copolymerisation: Selective Catalysis Delivering Alternating Copolymers. *Angew. Chem. Int. Ed.* **2021**, DOI: 10.1002/anie.202104495.
- (5) Gruszka, W.; Garden, J. A. Advances in Heterometallic Ring-Opening (Co)Polymerisation Catalysis. *Nat. Commun.* **2021**, *12* (1), 3252 - 3265.
- (6) Buchwalter, P.; Rosé, J.; Braunstein, P. Multimetallic Catalysis Based on Heterometallic Complexes and Clusters. *Chem. Rev.* **2015**, *115* (1), 28–126.
- (7) Longo, J. M.; Sanford, M. J.; Coates, G. W. Ring-Opening Copolymerization of Epoxides and Cyclic Anhydrides with Discrete Metal Complexes: Structure–Property Relationships. *Chem. Rev.* **2016**, *116* (24), 15167–15197.

- (8) Gao, Y.; Chen, X.; Zhang, J.; Chen, J.; Lohr, T. L.; Marks, T. J. Catalyst Nuclearity Effects on Stereo- and Regioinduction in Pyridylamidohafnium-Catalyzed Propylene and 1-Octene Polymerizations. *Macromolecules* **2018**, *51* (6), 2401–2410.
- (9) He, X.; Wang, Y.; Yuan, D.; You, H.; Yao, Y. Synthesis, Characterization, and Catalytic Study of Amine-Bridged Bis(Phenolato) Co(II) and Co(II/III)-M(I) Complexes (M = K or Na). *Inorg. Chem.* **2021**, *60* (15), 11521–11529.
- (10) Deacy, A. C.; Durr, C. B.; Garden, J. A.; White, A. J. P.; Williams, C. K. Groups 1, 2 and Zn(II) Heterodinuclear Catalysts for Epoxide/CO₂ Ring-Opening Copolymerization. *Inorg. Chem.* **2018**, *57* (24), 15575–15583.
- (11) Deacy, A. C.; Durr, C. B.; Williams, C. K. Heterodinuclear Complexes Featuring Zn(II) and M = Al(III), Ga(III) or In(III) for Cyclohexene Oxide and CO₂ Copolymerisation. *Dalton Trans.* **2019**, *49* (1), 223–231.
- (12) Deacy, A. C.; Durr, C. B.; Kerr, R. W. F.; Williams, C. K. Heterodinuclear Catalysts Zn(II)/M and Mg(II)/M, Where M = Na(I), Ca(II) or Cd(II), for Phthalic Anhydride/Cyclohexene Oxide Ring Opening Copolymerisation. *Catal. Sci. Technol.* **2021**, *11* (9), 3109–3118.
- (13) Zhu, Y.; Romain, C.; Williams, C. K. Sustainable Polymers from Renewable Resources. *Nature* **2016**, *540* (7633), 354–362.
- (14) Scharfenberg, M.; Hilf, J.; Frey, H. Functional Polycarbonates from Carbon Dioxide and Tailored Epoxide Monomers: Degradable Materials and Their Application Potential. *Advanced Functional Materials* **2018**, *28* (10), 1704302.

- (15) Anderson, T. S.; Kozak, C. M. Ring-Opening Polymerization of Epoxides and Ring-Opening Copolymerization of CO₂ with Epoxides by a Zinc Amino-Bis(Phenolate) Catalyst. *European Polymer Journal* **2019**, *120*, 109237.
- (16) Wang, Y.; Darensbourg, D. J. Carbon Dioxide-Based Functional Polycarbonates: Metal Catalyzed Copolymerization of CO₂ and Epoxides. *Coordination Chemistry Reviews* **2018**, *372*, 85–100.
- (17) Burkart, M. D.; Hazari, N.; Tway, C. L.; Zeitler, E. L. Opportunities and Challenges for Catalysis in Carbon Dioxide Utilization. *ACS Catal.* **2019**, *9* (9), 7937–7956.
- (18) Zhang, Y.-Y.; Wu, G.-P.; Darensbourg, D. J. CO₂-Based Block Copolymers: Present and Future Designs. *TRECHEM* **2020**, *2* (8), 750–763.
- (19) Langanke, J.; Wolf, A.; Hofmann, J.; Böhm, K.; A. Subhani, M.; E. Müller, T.; Leitner, W.; Gürtler, C. Carbon Dioxide (CO₂) as Sustainable Feedstock for Polyurethane Production. *Green Chemistry* **2014**, *16* (4), 1865–1870.
- (20) Kuran, W.; Sobczak, M.; Listos, T.; Debek, C.; Florjanczyk, Z. New Route to Oligocarbonate Diols Suitable for the Synthesis of Polyurethane Elastomers. *Polymer* **2000**, *41* (24), 8531–8541.
- (21) Alagi, P.; Ghorpade, R.; Choi, Y. J.; Patil, U.; Kim, I.; Baik, J. H.; Hong, S. C. Carbon Dioxide-Based Polyols as Sustainable Feedstock of Thermoplastic Polyurethane for Corrosion-Resistant Metal Coating. *ACS Sustainable Chem. Eng.* **2017**, *5* (5), 3871–3881.
- (22) Xu, S.; Zhang, M. Synthesis and Characterization of a Novel Polyurethane Elastomer Based on CO₂ Copolymer. *Journal of Applied Polymer Science* **2007**, *104* (6), 3818–3826.

(23) Peña Carrodegua, L.; Chen, T. T.; Gregory, G.; Sulley, G.; Williams, C. High Elasticity, Chemically Recyclable, Thermoplastics from Bio-Based Monomers: Carbon Dioxide, Limonene Oxide and ϵ -Decalactone. *Green Chemistry* **2020**, *22* (23), 8298–8307.

(24) Sulley, G. S.; Gregory, G. L.; Chen, T. T. D.; Peña Carrodegua, L.; Trott, G.; Santmarti, A.; Lee, K.-Y.; Terrill, N. J.; Williams, C. K. Switchable Catalysis Improves the Properties of CO₂-Derived Polymers: Poly(Cyclohexene Carbonate-*b*- ϵ -Decalactone-*b*-Cyclohexene Carbonate) Adhesives, Elastomers, and Toughened Plastics. *J. Am. Chem. Soc.* **2020**, *142* (9), 4367–4378.

(25) Deacy, A. C.; Gregory, G. L.; Sulley, G. S.; Chen, T. T. D.; Williams, C. K. Sequence Control from Mixtures: Switchable Polymerization Catalysis and Future Materials Applications. *J. Am. Chem. Soc.* **2021**, *143* (27), 10021–10040.

(26) Paul, S.; Zhu, Y.; Romain, C.; Brooks, R.; Saini, P. K.; Williams, C. K. Ring-Opening Copolymerization (ROCOP): Synthesis and Properties of Polyesters and Polycarbonates. *Chem. Commun.* **2015**, *51* (30), 6459–6479.

(27) Gregory, G. L.; Sulley, G. S.; Carrodegua, L. P.; Chen, T. T. D.; Santmarti, A.; Terrill, N. J.; Lee, K.-Y.; Williams, C. K. Triblock Polyester Thermoplastic Elastomers with Semi-Aromatic Polymer End Blocks by Ring-Opening Copolymerization. *Chem. Sci.* **2020**, *11* (25), 6567–6581.

(28) Chen, T. T. D.; Carrodegua, L. P.; Sulley, G. S.; Gregory, G. L.; Williams, C. K. Bio-Based and Degradable Block Polyester Pressure-Sensitive Adhesives. *Angew. Chem. Int. Ed.* **2020**, *59* (52), 23450–23455.

- (29) Zhang, X.; Fevre, M.; Jones, G. O.; Waymouth, R. M. Catalysis as an Enabling Science for Sustainable Polymers. *Chem. Rev.* **2018**, *118* (2), 839–885.
- (30) Haider, T. P.; Völker, C.; Kramm, J.; Landfester, K.; Wurm, F. R. Plastics of the Future? The Impact of Biodegradable Polymers on the Environment and on Society. *Angew. Chem. Int. Ed.* **2019**, *58* (1), 50–62.
- (31) Satti, S. M.; Shah, A. A. Polyester-Based Biodegradable Plastics: An Approach towards Sustainable Development. *Lett. Appl. Microbiol.* **2020**, *70* (6), 413–430.
- (32) Artham, T.; Doble, M. Biodegradation of Aliphatic and Aromatic Polycarbonates. *Macromol. Biosci.* **2008**, *8* (1), 14–24.
- (33) Coates, G. W.; Getzler, Y. D. Y. L. Chemical Recycling to Monomer for an Ideal, Circular Polymer Economy. *Nat. Rev. Mat.* **2020**, *5*, 501–516.
- (34) Rahimi, A.; García, J. M. Chemical Recycling of Waste Plastics for New Materials Production. *Nature Reviews Chemistry* **2017**, *1* (6), 1–11.
- (35) Abel, B. A.; Lidston, C. A. L.; Coates, G. W. Mechanism-Inspired Design of Bifunctional Catalysts for the Alternating Ring-Opening Copolymerization of Epoxides and Cyclic Anhydrides. *J. Am. Chem. Soc.* **2019**, *141* (32), 12760–12769.
- (36) S, S.; Min, J. K.; Seong, J. E.; Na, S. J.; Lee, B. Y. A Highly Active and Recyclable Catalytic System for CO₂/Propylene Oxide Copolymerization. *Angew. Chem. Int. Ed.* **2008**, *47* (38), 7306–7309.

- (37) Noh, E. K.; Na, S. J.; S, S.; Kim, S.-W.; Lee, B. Y. Two Components in a Molecule: Highly Efficient and Thermally Robust Catalytic System for CO₂/Epoxide Copolymerization. *J. Am. Chem. Soc.* **2007**, *129* (26), 8082–8083.
- (38) Lidston, C. A. L.; Abel, B. A.; Coates, G. W. Bifunctional Catalysis Prevents Inhibition in Reversible-Deactivation Ring-Opening Copolymerizations of Epoxides and Cyclic Anhydrides. *J. Am. Chem. Soc.* **2020**, *142* (47), 20161–20169.
- (39) Deng, J.; Ratanasak, M.; Sako, Y.; Tokuda, H.; Maeda, C.; Hasegawa, J.; Nozaki, K.; Ema, T. Aluminum Porphyrins with Quaternary Ammonium Halides as Catalysts for Copolymerization of Cyclohexene Oxide and CO₂ : Metal–Ligand Cooperative Catalysis. *Chem. Sci.* **2020**, *11* (22), 5669–5675.
- (40) Plajer, A. J.; Williams, C. K. Heterotrimetallic Carbon Dioxide Copolymerization and Switchable Catalysts: Sodium Is the Key to High Activity and Unusual Selectivity. *Angew. Chem. Int. Ed.* **2021**, *60* (24), 13372–13379.
- (41) Nagae, H.; Aoki, R.; Akutagawa, S.; Kleemann, J.; Tagawa, R.; Schindler, T.; Choi, G.; Spaniol, T. P.; Tsurugi, H.; Okuda, J.; Mashima, K. Lanthanide Complexes Supported by a Trizinc Crown Ether as Catalysts for Alternating Copolymerization of Epoxide and CO₂: Telomerization Controlled by Carboxylate Anions. *Angew. Chem. Int. Ed.* **2018**, *57* (9), 2492–2496.
- (42) Asaba, H.; Iwasaki, T.; Hatazawa, M.; Deng, J.; Nagae, H.; Mashima, K.; Nozaki, K. Alternating Copolymerization of CO₂ and Cyclohexene Oxide Catalyzed by Cobalt–Lanthanide Mixed Multinuclear Complexes. *Inorg. Chem.* **2020**, *59* (12), 7928–7933.

- (43) Kember, M. R.; White, A. J. P.; Williams, C. K. Highly Active Di- and Trimetallic Cobalt Catalysts for the Copolymerization of CHO and CO₂ at Atmospheric Pressure. *Macromolecules* **2010**, *43* (5), 2291–2298.
- (44) Qin, J.; Xu, B.; Zhang, Y.; Yuan, D.; Yao, Y. Cooperative Rare Earth Metal–Zinc Based Heterometallic Catalysts for Copolymerization of CO₂ and Cyclohexene Oxide. *Green Chem.* **2016**, *18* (15), 4270–4275.
- (45) Hua, L.; Li, B.; Han, C.; Gao, P.; Wang, Y.; Yuan, D.; Yao, Y. Synthesis of Homo- and Heteronuclear Rare-Earth Metal Complexes Stabilized by Ethanolamine-Bridged Bis(Phenolato) Ligands and Their Application in Catalyzing Reactions of CO₂ and Epoxides. *Inorg. Chem.* **2019**, *58* (13), 8775–8786.
- (46) Cui, L.; Ren, B.-H.; Lu, X.-B. Trinuclear Salphen–Chromium(III)Chloride Complexes as Catalysts for the Alternating Copolymerization of Epoxides and Cyclic Anhydrides. *J Polym. Sci.* **2021**, *59*, 1821–1828.
- (47) Duan, R.; Hu, C.; Sun, Z.; Zhang, H.; Pang, X.; Chen, X. Conjugated Tri-Nuclear Salen-Co Complexes for the Copolymerization of Epoxides/CO₂ : Cocatalyst-Free Catalysis. *Green Chemistry* **2019**, *21* (17), 4723–4731.
- (48) Duan, R.; Zhou, Y.; Huang, Y.; Sun, Z.; Zhang, H.; Pang, X.; Chen, X. A Trinuclear Salen–Al Complex for Copolymerization of Epoxides and Anhydride: Mechanistic Insight into a Cocatalyst-Free System. *Chem. Commun.* **2021**, *57* (1), 133–136.

- (49) Su, Y.-C.; Ko, B.-T. Alternating Copolymerization of Carbon Dioxide with Epoxides Using Highly Active Dinuclear Nickel Complexes: Catalysis and Kinetics. *Inorg. Chem.* **2021**, *60* (2), 852–865.
- (50) Deacy, A. C.; Kilpatrick, A. F. R.; Regoutz, A.; Williams, C. K. Understanding Metal Synergy in Heterodinuclear Catalysts for the Copolymerization of CO₂ and Epoxides. *Nat. Chem.* **2020**, *12* (4), 372–380.
- (51) Rosetto, G.; Deacy, A. C.; Williams, C. K. Mg(II) Heterodinuclear Catalysts Delivering Carbon Dioxide Derived Multi-Block Polymers. *Chem. Sci.* **2021**, DOI: 10.1039/D1SC03856G.
- (52) Lindeboom, W.; Fraser, D. A. X.; Durr, C. B.; Williams, C. K. Heterodinuclear Zn(II), Mg(II) or Co(III) with Na(I) Catalysts for Carbon Dioxide and Cyclohexene Oxide Ring Opening Copolymerizations. *Chem. A Eur. J.* **2021**, *27*, 12224–12231.
- (53) Deacy, A. C.; Moreby, E.; Phanopoulos, A.; Williams, C. K. Co(III)/Alkali-Metal(I) Heterodinuclear Catalysts for the Ring-Opening Copolymerization of CO₂ and Propylene Oxide. *J. Am. Chem. Soc.* **2020**, *142* (45), 19150–19160.
- (54) Bok, T.; Yun, H.; Lee, B. Y. Bimetallic Fluorine-Substituted Anilido–Aldimine Zinc Complexes for CO₂/(Cyclohexene Oxide) Copolymerization. *Inorg. Chem.* **2006**, *45* (10), 4228–4237.
- (55) Kissling, S.; Lehenmeier, M. W.; Altenbuchner, P. T.; Kronast, A.; Reiter, M.; Deglmann, P.; Seemann, U. B.; Rieger, B. Dinuclear Zinc Catalysts with Unprecedented Activities for the Copolymerization of Cyclohexene Oxide and CO₂. *Chem. Commun.* **2015**, *51* (22), 4579–4582.

- (56) Trott, G.; Garden, J. A.; Williams, C. K. Heterodinuclear Zinc and Magnesium Catalysts for Epoxide/CO₂ Ring Opening Copolymerizations. *Chem. Sci.* **2019**, *10* (17), 4618–4627.
- (57) Akine, S.; Utsuno, F.; Piao, S.; Orita, H.; Tsuzuki, S.; Nabeshima, T. Synthesis, Ion Recognition Ability, and Metal-Assisted Aggregation Behavior of Dinuclear Metallohosts Having a Bis(Saloph) Macrocyclic Ligand. *Inorg. Chem.* **2016**, *55* (2), 810–821.
- (58) Sakata, Y.; Tamiya, M.; Okada, M.; Akine, S. Switching of Recognition First and Reaction First Mechanisms in Host–Guest Binding Associated with Chemical Reactions. *J. Am. Chem. Soc.* **2019**, *141* (39), 15597–15604.
- (59) Sakata, Y.; Murata, C.; Akine, S. Anion-Capped Metallohost Allows Extremely Slow Guest Uptake and on-Demand Acceleration of Guest Exchange. *Nat Commun* **2017**, *8* (1), 16005.
- (60) Sakata, Y.; Kobayashi, S.; Akine, S. Two-Step Modulation of Ion Recognition Using a Bis(Saloph)-Macrocyclic Host Having a 24-Crown-8-like Cavity. *Chem. Commun.* **2017**, *53* (47), 6363–6366.
- (61) Deacy, A. C.; Reis, N.; Rosetto, G.; Williams C. K., *in preparation*.
- (62) Schütze, M.; Dechert, S.; Meyer, F. Highly Active and Readily Accessible Proline-Based Dizinc Catalyst for CO₂/Epoxide Copolymerization. *Chem. Eur. J.* **2017**, *23* (65), 16472–16475.
- (63) Cui, D.; Nishiura, M.; Hou, Z. Alternating Copolymerization of Cyclohexene Oxide and Carbon Dioxide Catalyzed by Organo Rare Earth Metal Complexes. *Macromolecules* **2005**, *38* (10), 4089–4095.

- (64) Saini, P. K.; Romain, C.; Williams, C. K. Dinuclear Metal Catalysts: Improved Performance of Heterodinuclear Mixed Catalysts for CO₂-Epoxide Copolymerization. *Chem. Commun.* **2014**, 50 (32), 4164–4167.
- (65) Lin, L.; Liang, J.; Xu, Y.; Wang, S.; Xiao, M.; Sun, L.; Meng, Y. Fully Alternating Sustainable Polyesters from Epoxides and Cyclic Anhydrides: Economical and Metal-Free Dual Catalysis. *Green Chem.* **2019**, 21 (9), 2469–2477.
- (66) Li, J.; Liu, Y.; Ren, W.-M.; Lu, X.-B. Asymmetric Alternating Copolymerization of Meso-Epoxides and Cyclic Anhydrides: Efficient Access to Enantiopure Polyesters. *J. Am. Chem. Soc.* **2016**, 138 (36), 11493–11496.
- (67) Shi, Z.; Jiang, Q.; Song, Z.; Wang, Z.; Gao, C. Dinuclear Iron(III) Complexes Bearing Phenylene-Bridged Bis(Amino Triphenolate) Ligands as Catalysts for the Copolymerization of Cyclohexene Oxide with Carbon Dioxide or Phthalic Anhydride. *Polym. Chem.* **2018**, 9 (38), 4733–4743.
- (68) Xie, R.; Zhang, Y.-Y.; Yang, G.-W.; Zhu, X.-F.; Li, B.; Wu, G.-P. Record Productivity and Unprecedented Molecular Weight for Ring-Opening Copolymerization of Epoxides and Cyclic Anhydrides Enabled by Organoboron Catalysts. *Angew. Chem. Int. Ed.* **2021**, 60, 19253–19261
- (69) Diment, W. T.; Gregory, G. L.; Kerr, R. W. F.; Phanopoulos, A.; Buchard, A.; Williams, C. K. Catalytic Synergy Using Al(III) and Group 1 Metals to Accelerate Epoxide and Anhydride Ring Opening Copolymerizations. *submitted*

(70) Diment, W. T.; Stöber, T.; Kerr, R. W. F.; Phanopoulos, A.; Durr, C. B.; Williams, C. K. Ortho-Vanillin Derived Al(III) and Co(III) Catalyst Systems for Switchable Catalysis Using ϵ -Decalactone, Phthalic Anhydride and Cyclohexene Oxide. *Catal. Sci. Technol.* **2021**, *11* (5), 1737–1745.

(71) Sarazin, Y.; Carpentier, J.-F. Discrete Cationic Complexes for Ring-Opening Polymerization Catalysis of Cyclic Esters and Epoxides. *Chem. Rev.* **2015**, *115* (9), 3564–3614.

(72) Hannant, M. D.; Schormann, M.; Bochmann, M. Synthesis and Catalytic Activity of Three-Coordinate Zinc Cations. *Dalton Trans.* **2002**, *22*, 4071–4073.

(73) Ungpittagul, T.; Jaenjai, T.; Roongcharoen, T.; Namuangruk, S.; Phomphrai, K. Unprecedented Double Insertion of Cyclohexene Oxide in Ring-Opening Copolymerization with Cyclic Anhydrides Catalyzed by a Tin(II) Alkoxide Complex. *Macromolecules* **2020**, *53* (22), 9869–9877.

(74) Yuntawattana, N.; Gregory, G. L.; Carrodegua, L. P.; Williams, C. K. Switchable Polymerization Catalysis Using a Tin(II) Catalyst and Commercial Monomers to Toughen Poly(l-Lactide). *ACS Macro Lett.* **2021**, *10* (7), 774–779.

(75) Sakata, Y.; Okada, M.; Tamiya, M.; Akine, S. Post-Metalation Modification of a Macrocyclic Dicobalt(III) Metallohost by Site-Selective Ligand Exchange for Guest Recognition Control. *Chem. Eur. J.* **2020**, *26* (34), 7595–7601.

(76) Fieser, M. E.; Sanford, M. J.; Mitchell, L. A.; Dunbar, C. R.; Mandal, M.; Van Zee, N. J.; Urness, D. M.; Cramer, C. J.; Coates, G. W.; Tolman, W. B. Mechanistic Insights into the

Alternating Copolymerization of Epoxides and Cyclic Anhydrides Using a (Salph)AlCl and Iminium Salt Catalytic System. *J. Am. Chem. Soc.* **2017**, *139* (42), 15222–15231.

(77) Gade, L. H. *Koordinationschemie*; 344 - 345, John Wiley & Sons, **2012**.

(78) Klaus, S.; Lehenmeier, M. W.; Herdtweck, E.; Deglmann, P.; Ott, A. K.; Rieger, B. Mechanistic Insights into Heterogeneous Zinc Dicarboxylates and Theoretical Considerations for CO₂–Epoxide Copolymerization. *J. Am. Chem. Soc.* **2011**, *133* (33), 13151–13161.

(79) Xia, W.; Salmeia, K. A.; Vagin, S. I.; Rieger, B. Concerning the Deactivation of Cobalt(III)-Based Porphyrin and Salen Catalysts in Epoxide/CO₂ Copolymerization. *Chem. Eur. J.* **2015**, *21* (11), 4384–4390.

(80) Ren, W.-M.; Liu, Z.-W.; Wen, Y.-Q.; Zhang, R.; Lu, X.-B. Mechanistic Aspects of the Copolymerization of CO₂ with Epoxides Using a Thermally Stable Single-Site Cobalt(III) Catalyst. *J. Am. Chem. Soc.* **2009**, *131* (32), 11509–11518.

(81) Yang, G.-W.; Zhang, Y.-Y.; Xie, R.; Wu, G.-P. Scalable Bifunctional Organoboron Catalysts for Copolymerization of CO₂ and Epoxides with Unprecedented Efficiency. *J. Am. Chem. Soc.* **2020**, *142* (28), 12245–12255.

(82) Gentner, T. X.; Mulvey, R. E. Alkali-Metal Mediation: Diversity of Applications in Main-Group Organometallic Chemistry. *Angew. Chem. Int. Ed.* **2021**, *60* (17), 9247–9262.

(83) Ji, H.-Y.; Song, D.-P.; Wang, B.; Pan, L.; Li, Y.-S. Organic Lewis Pairs for Selective Copolymerization of Epoxides with Anhydrides to Access Sequence-Controlled Block Copolymers. *Green Chem.* **2019**, *21* (22), 6123–6132.

Synopsis: A series of heterotrimetallic catalysts for carbon dioxide/epoxide or cyclic anhydride/epoxide ring-opening copolymerizations reveal some of the structural requirements for activity and linkage selectivity. The most active catalyst combines abundant and low toxicity metals such as Zn(II), Mg(II) and Na(I) and can also catalyse epoxide ring opening polymerization to furnish various block polymers.

